1998

Observation of the seismic nucleation phase in the Ridgecrest, California, earthquake sequence

William L. Ellsworth
U.S. Geological Survey

Gregory C. Beroza
Stanford University

GEOPHYSICAL RESEARCH LETTERS, VOL. 25, NO. 3, PAGES 401-404, FEBRUARY 1, 1998

Observation of the seismic nucleation phase in the Ridgecrest, California, earthquake sequence

William L. Ellsworth
U.S. Geological Survey, Menlo Park, California

Gregory C. Beroza
Stanford University, Stanford, California

Abstract. Near-source observations of five M 3.8–5.2 earthquakes near Ridgecrest, California are consistent with the presence of a seismic nucleation phase. These earthquakes start abruptly, but then slow or stop before rapidly growing again toward their maximum rate of moment release. Deconvolution of instrument and path effects by empirical Green's functions demonstrates that the initial complexity at the start of the earthquake is a source effect. The rapid growth of the *P*-wave arrival at the start of the seismic nucleation phase supports the conclusion of *Mori and Kanamori* [1996] that these earthquakes begin without a magnitude-scaled slow initial phase of the type observed by *Iio* [1992, 1995].

Introduction

Both theory and laboratory simulations of earthquakes propose that a fault must slide stably within a finite nucleation zone before dynamic rupture can occur [e.g., *Dieterich*, 1979; *Das and Scholz*, 1982]. Such slow deformation, however, has proven to be exceedingly difficult to detect, and the most reliable deformation observations can only bound the pre-earthquake moment release to be no more than about 0.2–2% of the seismic moment [e.g., *Johnston et al.*, 1994].

An alternative approach to studying the aseismic earthquake nucleation process examines the initial seismic motions during the high-speed rupture for evidence of processes that prepare the fault for failure. Near-source recordings of earthquakes made on high-sensitivity and wide dynamic range digital instruments with strictly causal response show that the dynamic motion starts suddenly, but with an interval of relatively weak motion we have called the seismic nucleation phase [*Ellsworth and Beroza*, 1995; *Beroza and Ellsworth*, 1996]. This dynamic phase contains on average 0.5% of the total moment, but lasts on average for about 1/6 of the duration of the remainder of the earthquake. The seismic moment rate of the earthquake typically slows during the seismic nucleation phase before increasing rapidly (breakaway phase), as the event grows toward its maximum rate of moment release.

Our observations were drawn from recordings made around the world, spanning the magnitude range from M 1 to 8. Such near-source recordings, however, are relatively uncommon, raising the possibility of a sampling bias in the observations. Recently, *Mori and Kanamori* [1996] examined about 50 M = 0.5–5.2 events recorded on high gain analog instruments in the epicentral region of earthquakes that occurred near Ridgecrest, California in 1995–1996. They concluded that there was no evidence in those data for magnitude-dependent "precursory" rupture initiation process.

In this paper, we examine initial seismic moment rate of five of the largest Ridgecrest events with near-source data, and demonstrate that these earthquakes begin with the same type of seismic nucleation phase we have previously documented, as described above.

Ridgecrest Earthquakes and Seismograms

From the late summer of 1995 through the spring of 1996, a protracted earthquake sequence occurred in eastern California near the town of Ridgecrest [*Hauksson et al.*, 1995]. The sequence included several M 5 and numerous M 3 and 4 earthquakes. The sustained nature of the seismicity was recognized by *Mori and Kanamori* [1996] and *Hough* [1997] as an opportunity to deploy temporary seismograph stations atop the source area to record details of the earthquake source process.

Mori and Kanamori [1996] installed a dual-gain, 3-component 1 Hz velocity geophone with analog telemetry at station RGC (Figure 1). Seismograms were collected by the

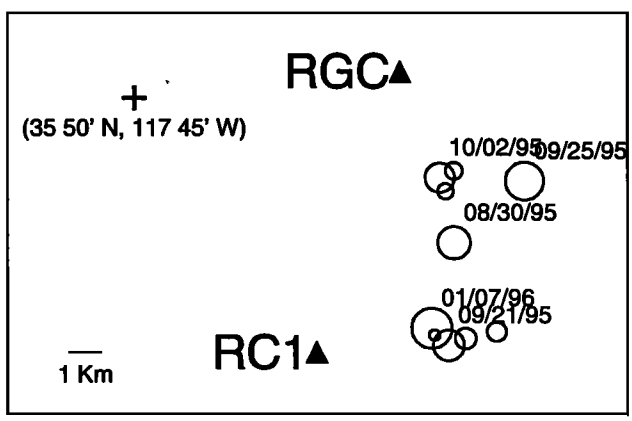

Figure 1. Map showing epicentral region of the 1995–1996 Ridgecrest, California earthquake sequence. Plotted earthquakes are analyzed in this paper. Symbol size proportional to magnitude. Triangles are temporary stations.

Paper number 97GL53700.
0094-8534/98/97GL-53700$05.00

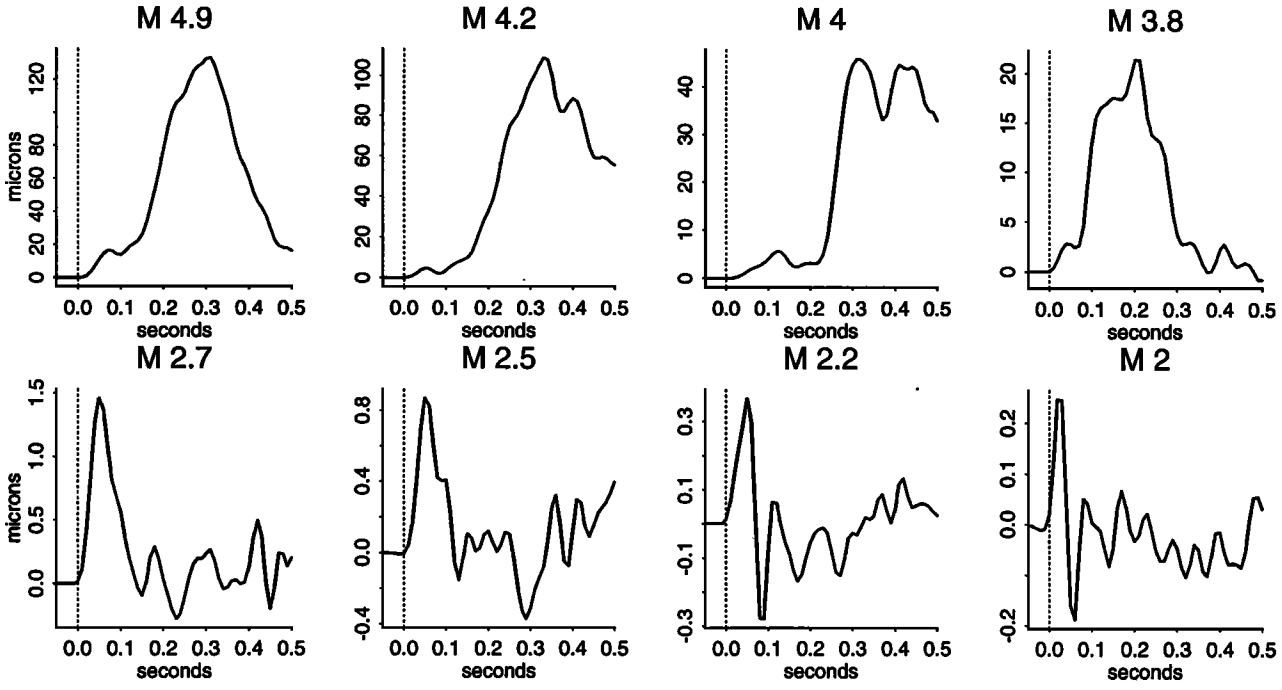

Figure 2. Displacement seismograms for earthquakes recorded at digital accelerometer station RC1. Dashed vertical line at marks the *P*-wave arrival. The seismic nucleation phase is clearly visible at the beginning of the larger events (top row), but cannot be resolved, if present, for smaller events (bottom row) due to propagation effects and sample rate.

same computer system used to record the analog Southern California Seismic Network. The seismograms were sampled at 100 Hz, and typically clip the low gain component on the initial *P* wave for events $M \geq 3$. A force balance accelerometer (FBA) was also installed at RGC, from which we have recovered useful data for only one event. Mori and Kanamori focussed on the initial *P*-wave onset, and examined only the first 0.05 s of the seismogram. They proposed that the shape of the initial onset could be satisfactorally explained by a self-similarly growing rupture after correction for a path attenuation of $t^* = 0.02$ s, or an equivalent path-averaged *P*-wave *Q* of about 100.

Hough [1997] installed an FBA at station RC1, recorded by a 16 bit digital data logger that does not employ FIR filters. Hough estimated average source properties in the frequency domain using empirical Green's function (EGF) deconvolution by spectral division. The spectral division method is not suitable for analyzing the initial portions of the moment-rate function, which is the focus of our study.

Analysis of the initial *P*-wave for Ridgecrest earthquakes is complicated by several factors that we have previously been careful to avoid. Site conditions at both RGC and RC1 are poor, with about 1.6 km of low *Q* sediments beneath the recording sites, leading to strong attenuation of the seismograms [*Hough*, 1997] despite the short hypocentral range. Seismic nucleation phases for $M \leq 3$ events, if present and following the same scaling reported earlier should last for only 0.01 s or less [*Ellsworth and Beroza*, 1995], and would be unobservable at either RGC or RC1 due to the combined effects of the 25 Hz frequency antialias filter and anelastic attenuation. For larger magnitude events, our predicted nucleation phase should be observable. *P*-wave arrivals for $M \geq 3$ events on the low-gain vertical seismograms at RGC usually clip within 0.03–0.06 s of onset and the few on-scale points merely track the clipping response of the analog telemetry system. The 16-bit digital accelerograms from RC1 are on-scale, but only have useable signal to noise ratios for events $M \cong 2$ or larger. In view of these limitations, we focus our attention on the largest events recorded at RC1 and the few events with limited on-scale data at RGC (Table 1).

Analysis Procedures

Accelerograms from RC1 were integrated to displacement in the time domain. Displacement seismograms for the four largest events and four nearby smaller events (Figure 2) display excellent data quality over a wide frequency band. Note the approximately $100x$ change in displacement amplitude for a magnitude difference of 2 units, as is expected from constant stress drop scaling.

Two of the earthquakes recorded at RC1 have EGF events [*Hough*, 1997] suitable for use to determine the moment rate function by deconvolving the path effects and the instrument response. The other RC1 events did not have acceptable EGF events. We also use deconvolution to determine the initial moment rate for the unclipped beginnings of the M 5.2 event recorded at RGC. The deconvolution is

Table 1. Measured Seismic Nucleation Properties

Event		M	Nucleation	Nucleation
		Duration (s)	Moment (%)	
08/30/95	15:29	4.2	0.13	0.1
09/21/95	23:48	4.0	0.15	3
09/25/95	04:47	4.9	0.10	3
10/02/95	00:10	3.8	0.06	2
01/07/96	14:32	5.2	>0.04	>0.02

performed as an inverse problem in the time domain, with the solution regularized by minimizing the curvature of the moment rate function. In the time domain, convolution may be written as a matrix equation $s = Gm$ where the columns of G contain time-shifted copies of the EGF and zero above the main diagonal, s is the mainshock seismogram, and m is the moment rate function. Although we can always solve this system of equations, its solution may depend critically on small errors in either s or g. Regularization is supplied by requiring m to be smooth by minimizing the norm of a second difference operator, Dm. The relative weight of the two systems of equations is controlled through a trade-off parameter, ϵ. We also require the moment rate to be non-negative. Thus, the goal is to Minimize $\left(\| s - Gm \|^2 + \epsilon \| Dm \|^2\right)$ subject to $m \geq 0$. The exact least-squares solution to this problem is determined using non-negative least-squares, and the optimum value of ϵ minimizes the Studentized cross validation residual [*Rousseeuw and Leroy*, 1987].

Results

The initial P-wave arrivals for both the $M \cong 4$ and $M \cong 2$ events recorded at RC1 (Figure 2) are impulsive. The displacement exceeds 0.1 micron within 0.01–0.03 seconds in all cases. The pulse shapes for the $M \cong 2$ events are quite simple, and rise to their peak values without any complexity or delay. In contrast, the $M \cong 4$ events all display a local maximum near their beginning before rising to their peak value. This is precisely the behavior that we have named the seismic nucleation phase. Because the pulse shapes for the M 2 events lack large secondary arrivals, it is likely that the complexity apparent at the beginning of the four larger events is a source effect and not a path effect. This conclusion can be tested by removing the path effects by deconvolving suitable EGF from the original seismograms.

Moment rate functions obtained by deconvolution (Figure 3) display essentially the same features as seen in the displacement seismograms. Both events have distinct, eventful beginnings that are weak relative to the moment rate that follows, and are consistent with our earlier observations (Table 1).

The beginning of the October 2, 1995 M 3.8 was also recorded on-scale at RGC on the vertical FBA and radial (N–S) horizontal seismometer (Figure 4). The onset of motion on these two low-gain components agree, but are clearly delayed relative to the high-gain vertical. The interval between the two arrivals of 0.03 s is half that observed at RC1. Since the two stations are located off the opposite ends of the strike slip fault activated during this sequence [*Hauksson et al.*, 1995], the difference might be due to spatial separation between the two sources if the second pulse initiated 0.045 s after and 100 m to the north of the initial hypocenter.

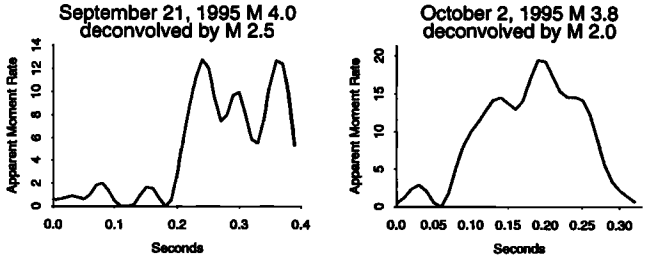

Figure 3. Moment rate functions obtained by time domain deconvolution of empirical Green's function events for two events recorded by RC1, in units of their respective empirical Green's function events of M 2.5 and 2.0. The moment rate functions display a distinct, hesitant beginning named the seismic nucleation phase by *Ellsworth and Beroza* [1995].

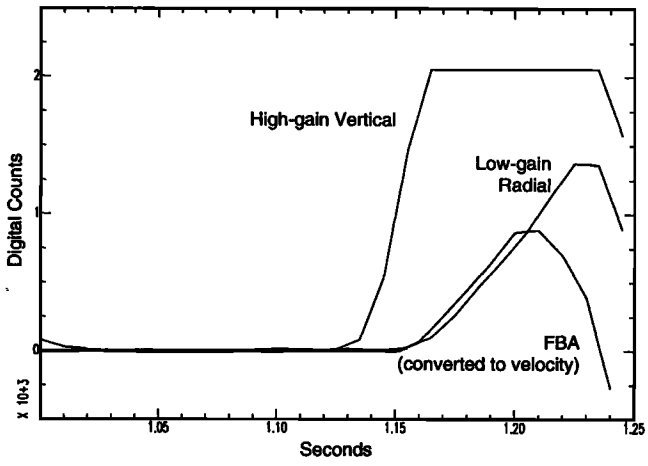

Figure 4. Details of P-wave arrival at RGC for October 2, 1995 M 3.8. High gain vertical and low gain radial components shown in digital counts as recorded. Vertical FBA shown as velocity seismogram with the same instrumental response.

The last large earthquake in the sequence, M 5.2, occurred on January 7, 1996 after RC1 was removed. Recordings on RGC (Figure 5a) show a prominent interruption in the seismogram about 0.06 s after the initial arrival on the low gain vertical and radial horizontal (N–S) components. Although this event was also studied by *Mori and Kanamori* [1996], this feature does not appear in their Figure 2, which was restricted to the first 0.05 seconds of the earthquake. Even though only a few samples of unclipped seismogram are available, this is sufficient for time domain EGF deconvolution. The results support the existence of a weak, hesitant start to this event (Figure 5b), and places lower bounds on its duration and seismic moment (Table 1).

Discussion and Conclusions

The nucleation process of five largest events, M 3.8–5.2, recorded by temporary stations at Ridgecrest are consistent with our earlier description of the seismic nucleation phase [*Ellsworth and Beroza*, 1995]. The moment rate for each event begins abruptly, but slows or halts before growing rapidly toward the peak moment release rate. The duration of the seismic nucleation phase [Table 1], as well as its moment, follow the same scaling relations with seismic moment of the entire earthquake [*Beroza and Ellsworth*, 1996].

Although the seismic nucleation moments are a small fraction of the respective main shock moments [Table 1], they have moments equivalent to earthquakes of M 2.2–3.9. The observed abrupt beginning of the initial P-wave is consistent with the radiation expected from events of this magnitude. In other words, the nucleating event has the appearance of a small earthquake. The rapid start for these events

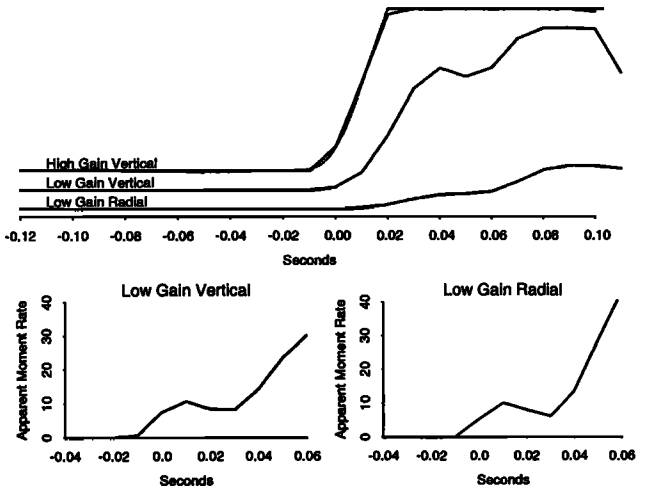

Figure 5. Details of *P*-wave arrival at RGC for January 7, 1996 M 5.2 (top). Clipping level is 2048 counts for the high gain vertical (16× relative gain), low gain vertical (1×) and low gain radial (1/8×). Note how high gain channel follows clipping response of electronics (dashed line). Moment rate function obtained by empirical Green's function deconvolution from low gain components in units of the M 1.4 Green's function event (bottom).

runs counter to the observations of a slow initial phase for M 0–2 recorded at high Q sites at very high sample rates by Iio in Japan [*Iio*, 1992, 1995]. It is possible that a gradual beginning of very short duration (< 0.01 s) could be present for Ridgecrest earthquakes, as such a process would not be observable in these data. However, it is clear from the high-gain data that such a phase does not scale systematically with magnitude, as it would be observable for $M \geq 4$ events at RGC [*Mori and Kanamori*, 1996].

So what are the implications of our observations for the earthquake nucleation process? We believe that the question is not if a seismic nucleation phase exists, but rather what it implies about the physics of nucleation. Many earthquakes initiate with a weak hesitiant beginning that is followed by a rapid increase in moment release rate.

We have suggested two extreme models that appear to be consistent with the data [*Ellsworth and Beroza*, 1995]. The preslip model proposes that aseismic slip occurs in a confined zone, within which the dynamic instability will begin. Slip within this confined zone creates localized stress concentrations that generate the initial, irregular far-field signal that we identify as the seismic nucleation phase when they rupture at the start of the dynamic event. *Fukuyama and Madariaga* [1997] have recently presented dynamic rupture models that begin with relatively weak radiation during initial rupture of a preslip zone. In their models, the initial radiation is controlled by the details of the stress field surrounding the preslip zone and the location of the initial hypocenter.

The alternative cascade model proposes that the irregular start to an earthquake represents a self-triggering progression of events of ever increasing size that is unrelated to an aseismic preparation process. The source of the heterogenity observed in the seismogram must arise through another means, such as the intrinsic geometric complexity of the fault. Given the intense, swarming nature of seismicity during this sequence including the frequent occurrence of foreshocks, the nucleation behavior of these M 3.8–5.2 earthquakes is as consistent with the cascade model as it is with the preslip model. In particular, the multiple-event character of the beginning of the September 21 M 4.0 earthquake (Figure 3) may be interpreted as a rapid succession of at least 3 $M \cong 2.5$ foreshocks. Although we cannot as yet distinguish between the two end member models, foreshocks themselves do not appear to be a simple cascade driven by elastic stress transfer from unbroken to broken parts of the fault [*Dodge et al.*, 1996].

Acknowledgments. We thank Sue Hough and Jim Mori for assistance in obtaining their data and many useful discussions. John VanSchaack helped clarify the clipping response of the analog telemetry system. We thank Sue Hough, Sharon Kedar, and John Vidale for helpful reviews. G. B. was supported by USGS grant 1434-HQ-96-GR-02716.

References

Beroza, G. C., and W. L. Ellsworth, Properties of the seismic nucleation phase, *Tectonophysics, 261*, 209–227, 1996.

Dieterich, J. H., Modelling of rock friction: 1 Experimental results and constitutive equations, *J. Geophys. Res, 84*, 2161–2168, 1979.

Das, S., and C. H. Scholz, Theory of time-dependent rupture in the Earth, *J. Geophys. Res., 86*, 6039–6051, 1981.

Dodge, D. A., G. C. Beroza, and W. L. Ellsworth, Detailed observations of California foreshock sequences: Implications for the earthquake initiation process, *J. Geophys. Res., 101*, 22,371–22,392, 1996.

Ellsworth, W. L., and G. C. Beroza, Seismic evidence for a seismic nucleation phase, *Science, 268*, 851–855, 1995.

Fukuyama, E., and R. Madariaga, Dynamic rupture of a planar fault in 3D: Friction and rupture initiation (abs.), *Seismol. Res. Lett., 68*, 329–330.

Hauksson, E., K. Hutton, H. Kanamori, L. Jones, J. Mori, S. Hough, and G. Roquemore, Preliminary report on the 1995 Ridgecrest earthquake sequence in eastern California, *Seismol. Res. Lett, 64*, no. 6, 54–60, 1995.

Hough, S. E., Empirical Green's function analysis: Taking the next step, *J. Geophys. Res., 102*, 5369–5384, 1997.

Iio, Y., Slow initial phase of the *P*-wave velocity pulse generated by microearthquakes, *Geophys. Res. Lett., 19*, 477–480, 1992.

Iio, Y., Observation of the slow initial phase of microearthquakes: Implications for earthquake nucleation and propagation, *J. Geophys. Res., 100*, 15,333–15,349, 1995.

Johnston, M. J. S., A. T. Linde, and D. C. Agnew, Continuous borehole strain in the San Andreas fault zone before, during and after the 28 June 1992, M_w7.3 Landers, Califorina, earthquake, *Bull. Seismol. Soc. Am., 84*, 799–805, 1994.

Mori, J., and H. Kanamori, Initial rupture of earthquakes in the 1995 Ridgecrest, California sequence, *Geophys. Res. Lett., 23*, 2437–2440, 1996.

Rousseeuw, P. J., and A. M. Leroy, *Robust Regression and Outlier Detection*, 329 pp., John Wiley and Sons, New York, 1987.

W. L. Ellsworth, U.S. Geological Survey, 345 Middlefield Road, MS/977, Menlo Park, California 94025. (e-mail: ellswrth@andreas.wr.usgs.gov)

G. C. Beroza, Department of Geophysics, Stanford University, Stanford, California 94305. (e-mail: beroza@pangea.stanford.edu)

(Received July 16, 1997; revised December 2, 1997; accepted December 8, 1997.)